



Optimisation of heat treatment of Al–Cu–(Mg–Ag) cast alloys

Mohammadreza Zamani¹ · Stefania Toschi² · Alessandro Morri² · Lorella Ceschini² · Salem Seifeddine¹

Received: 15 January 2019 / Accepted: 15 August 2019 / Published online: 29 August 2019
© The Author(s) 2019

Abstract

The optimisation of heat treatment parameters for Al–Cu–(Mg–Ag) cast alloys (2xxx) having different microstructural scales was investigated. Thermo-Calc software was used to design optimal alloy compositions. Differential scanning calorimetry (DSC), scanning electron microscopy and wavelength-dispersive spectroscopy technique were employed to determine proper solution heat treatment temperature and homogenisation time as well as incidence of incipient melting. Proper artificial ageing temperature for each alloy was identified using DSC analysis and hardness measurement. Microstructural scale had a pronounced influence on time and temperature required for complete dissolution of Al₂Cu and homogenisation of Cu solute atoms in the α -Al matrix. Refined microstructure required only one-step solution treatment and relatively short solution treatment of 10 h to achieve dissolution and homogenisation, while coarser microstructures desired longer time. Addition of Mg to Al–Cu alloys promoted the formation of phases having a rather low melting temperature which demands multi-step solution treatment. Presence of Ag decreases the melting temperature of intermetallics (beside Al₂Cu) and improvement in age-hardening response. Peak-aged temperature is primarily affected by the chemical composition rather than the microstructural scale.

Keywords Coarseness of microstructure · Cast Al–Cu alloys · Thermal treatment · Solution treatment · Artificial ageing · DSC · Solidification rate

Introduction

2xxx family of aluminium casting alloys are age hardenable, based on Al–Cu system, which offers high strength and hardness at ambient and elevated temperatures [1, 2]. Replacement of these alloys with ferrous components in the vehicle power trains (e.g. cylinder heads and engine blocks) inscribed lightweighting achievement in the automotive industry [2, 3]. Addition of Cu and Mg to Al strengthens the alloy not only through a solid solution strengthening but also in substantial dispersion strengthening mechanism through the formation of Al₂Cu and Al₂CuMg phases by heat treatment [4]. For the first time in

1966, Polmear and Vietz [5] demonstrated that small additions of Ag improve age-hardening response in Al–Cu–Mg alloys, with a rather high Cu/Mg ratio, due to changes in the common precipitation. Thin plates of finely dispersed Ω phase form on the [6] α -Al planes of the silver-containing alloys instead of the θ'' and θ' precipitates on the α -Al {111} planes during artificial ageing [7, 8].

Substantial improvement in the strength of Al–Cu–(Mg–Ag) alloys can be obtained by precipitating large amounts of θ' and Ω phases through heat treatment [9]. The highest rate of precipitation occurs when all secondary phases (Al₂Cu, Al₂CuMg, etc.) which are formed during solidification are entirely dissolved and atoms of alloying elements (e.g. Cu and Mg) are homogenised in the α -Al matrix during the solution heat treatment (SHT) [10]. Lowered solution temperature and/or short solutionising time do not ensure complete dissolution of phases and homogenisation of Cu atoms in the Al matrix. On the other hand, elevated solution temperature and prolonged SHT result in the occurring of incipient melting of phases and wasting of energy, respectively [10]. Incipient melting harms mechanical properties, and therefore, it is crucial to

✉ Mohammadreza Zamani
mohammadreza.zamani@ju.se

¹ Department of Materials and Manufacturing, School of Engineering, Jönköping University, 551 11 Jönköping, Sweden

² Department of Industrial Engineering (DIN), Alma Mater Studiorum - University of Bologna, 40136 Bologna, Italy

choose the optimal SHT for sound microstructure and desired performance. Solution temperature controls the diffusion-based dissolution rate of Al_2Cu , while homogenisation time is primarily determined by diffusion distance [11]. Factors such as fraction, type and morphology of Al_2Cu phases also determine their dissolution rate [12, 13]. T6 heat treatment was commonly applied for Al–Cu–Mg–(Ag) alloys, consisting of SHT at a temperature range of 495–530 °C for various times from 2 to 22 h, quenching in the water at ambient temperature followed by artificial ageing at 150–180 °C for 8–24 h [14].

Masuku et al. [15] showed that a two-step SHT for a cast Al–5Cu–Mg–Ag alloy (2139) is needed to intercept incident of incipient melting. The first step is heating at a lower temperature for a short time (at ~ 515 °C for 5 h) to ensure dissolution of phases with a lower melting point than eutectic Al_2Cu . The second step at a temperature above 515 °C for 10 h is to dissolve the Al_2Cu phase. Moller et al. [16] instead proposed a two-step homogenisation/solution heat treatment: homogenisation at 490 °C for 24 h, followed by a SHT at 520 °C for 2 h, which successfully prevents the formation of incipient melting pores to a great extent in 2139 alloy. Daswa et al. [17] suggested a mix of three-step SHT coupled with controlled heating for 2139 alloy: controlled heating from 400 to 513 °C and holding at 513 °C for 2 h and eventually heating to 525 °C and holding for 16 h.

In order to transform the supersaturated solid solution structure (solution heat-treated) to the high-strength tempers characterised by strengthening precipitates, the temperature of artificial ageing is the key parameter. At the optimal ageing temperature, the alloy reaches the peak-ageing hardness value within an adequate time, while, on the other hand, lower temperatures require a relatively long time to reach the peak; at higher temperatures, precipitates turn into relatively large non-coherent particles offering low strength (over-aged) [18]. In previous works, Al–Cu–Mg–Ag alloys were artificially aged at a quite wide temperature range from 150 to 250 °C to identify the peak-ageing condition [19–22]. The peak-ageing temperature was changed by changes in concentration of Cu, Mg and Ag in the alloy [20]. This was understood by artificial ageing of various Al–Cu–Mg–Ag cast alloys at 160, 190 and 220 °C. Li et al. [23] suggested that a duplex ageing treatment for an Al–5Cu–0.4Mg–1Ag alloy resulted in further improvement in mechanical properties compared to conventional ageing. It was shown that ageing at 200 °C for 20 min followed by 165 °C for 20 h results in 3–7% higher peak-aged hardness compared to solo ageing at 165 °C for 20 h due to controlled competitive precipitation between Ω and θ' phases [23].

The solidification of cast components is a complex process where factors such as casting technology (e.g. sand

casting, permanent mould casting, etc.) and component geometry affect the extraction of heat during solidification which leads to variations in the size of microstructural features [24]. The cooling rate varies with the local thickness of the cast component: a high cooling rate results in a refined microstructural features, while lower cooling rates yield a coarser microstructure [13]. It was shown that the microstructural scale (coarseness of microstructure) in Al–Si alloys influences solution treatment mechanism [10] and artificial ageing response [25]. Refined particles require a significantly shorter time to dissolve rather than the coarse ones. Smaller α -Al dendrites provide a shorter distance for homogenisation of atomic elements over the matrix. Unlike heat treatment of Al–Si cast alloys, no detailed discussion about heat treatment of Al–Cu–(Mg–Ag) alloys is reported in the literature. Since the as-cast microstructural scale controls mechanical properties of castings [24], it is, therefore, a useful exercise to investigate the role of microstructural scale on solution heat treatment and artificial ageing of Al–Cu–(Mg–Ag) cast alloys.

The main aim of the present study is to identify proper temperature range and time for solution heat treatment and artificial ageing of Al–Cu–(Mg–Ag) alloys having different as-cast microstructural scales using differential scanning calorimetry analysis, microstructural characterisation and hardness testing. Alloy compositions were designed with optimal Cu/Mg ratio suiting SHT process and decrease the risk of incipient melting occurrence. The role of Mg and Ag addition, as well as variation in microstructural scale on SHT and artificial ageing, was discussed.

Experimental

Material

Three different Al–Cu-based alloys were produced by melting pure Al ingots (99.99% purity), pure Cu (99.99% purity), the Al–25Mg (mass%) and the Al–10Ag (mass%) master alloys. Composition of these alloys was determined using a SPECTROMAXx optical emission spectroscope, and the average chemical composition obtained from six measurements is presented in Table 1.

The melt was prepared in a resistance furnace at 750 °C in a silicon carbide-bonded graphite crucible coated with boron nitride by a commercial spray. No degassing treatment was applied during the melting process. The melt was gravity-die-casted in a 250 °C preheated copper die having six cylindrical fingers of 200 mm long and 10 mm diameter. The cast rods were then re-melted at 730 °C for 30 min under Ar atmosphere in a Bridgman furnace and then directionally solidified [13]. The furnace was mounted

Table 1 Detailed compositions of alloys in mass%

Target composition	Cu	Mg	Ag	Fe	Si	Other	Al
Al–4.3Cu	4.33	–	–	0.07	0.05	< 0.01	Bal.
Al–4.3Cu–0.7Mg	4.28	0.73	–	0.07	0.04	< 0.01	Bal.
Al–4.3Cu–0.7Mg–0.7Ag	4.36	0.71	0.70	0.07	0.04	< 0.01	Bal.

on a motorised lifting device, while the rods are in a stationary position. After the rods had been re-melted, the furnace was raised at a prescribed speed. The pulling speed of the furnace controls the solidification rate. In order to produce cast specimens with different microstructural scales, the pulling speed of the furnace was set to 0.03, 0.3 and 3 mm s⁻¹.

Thermal analysis

Differential scanning calorimetry (DSC) analyses were performed using a NETZSCH 404C Pegasus[®] instrument in a purified argon atmosphere with the scanning rate of 5 °C min⁻¹, from 30 to 600 °C in order to study phase transformations within the material during heating in the as-cast and solution-treated conditions. Cylinders of 5 mm diameter with a mass of 42.1 ± 0.1 mg were prepared. Three tests were performed for each condition. Characteristic temperatures were measured using NETZSCH Proteus Thermal Analysis software.

Microstructural analysis

A scanning electron microscope (SEM, JEOL 7001F) equipped with an energy-dispersive spectrometer (EDS) is used to identify different phases in the microstructure. In order to study solute concentration profiles and segregation of the alloy elements (Cu, Mg and Ag) across the α -Al grains, a SEM (TESCAN Lyra3) equipped with wavelength-dispersive X-ray spectroscopy (WDS) was employed. The reason for choosing the point analysis by WDS rather than EDS was obtaining better energy/wavelength resolution and peak/background ratio. Different electron beam voltages of 5, 10 and 20 kV were set for measurement of Mg, Ag and Cu, respectively. Samples that were solution-treated at given temperatures for different times were immediately quenched in water at 40 °C. For each condition, at least 18 analysis points were measured across the α -Al grains for each specimen. Three different specimens were investigated for each condition. Olympus image analyser was used to coordinate the measured point with respect to distance to the nearest particle (Fig. 1).

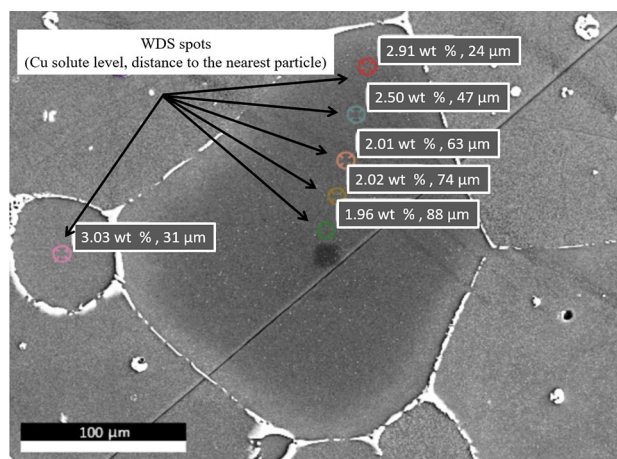


Fig. 1 Measured WDS spots across α -Al grains and their distance to nearest phases

Heat treatment and methodology

Specimens for heat treatment were cylinders of 1 cm long and 1 cm in diameter. Nabertherm LE2/11-R7 furnace was used for SHT process. The specimens were quenched in 40 °C water. Thereafter, they are artificially aged in Heraeus D-6450 furnace. The temperature of specimens was controlled using thermocouples inserted into each specimen during SHT and artificial ageing processes. The methodology of the heat treatment was based on choosing the temperature of SHT and artificial ageing with respect to onset temperature of melting of intermetallics and precipitates formation, respectively. The onset temperatures were identified through DSC analysis. A temperature of 15–20 °C below than onset temperature of melting Al₂Cu temperature was initially chosen for solution heat treatment. In the case of incomplete dissolution of intermetallics, SHT was carried out at relatively higher temperature. In the presence of peaks corresponding to melting of intermetallic compounds having lower melting temperature compared to Al₂Cu, two-step SHT was applied in order to prevent occurring of incipient melting of phases with lower melting temperatures. Sufficient SHT time was realised through characterisation of Cu solute level across the α -Al matrix through WDS analysis. Temperature of artificial ageing was chosen with respect to onset temperature of precipitates formation in order to find the temperature which gives the peak of hardness within the adequate time. Temperatures and time which were selected

for SHT and artificial ageing for different alloys are collated in Table 2.

Hardness test

The hardness of the alloys was measured by Vickers indentation at 2-kg load and a dwell time of 15 s, followed by ASTM E92 (2004) analysis procedures. For each condition, five measurements in identical locations from cylindrical sections were taken from three distinct specimens. The average hardness was calculated, and the standard error based on 95% confidence interval was reported. The hardness of the alloys was measured both in as-cast and in heat-treated conditions. The average hardness was calculated and plotted with respect to ageing time.

Results and discussion

Design of the alloys

The main strengthening phase in Al–Cu–(Mg–Ag)-based alloy is Al₂Cu which precipitates in the form of θ'' , θ' and Ω phases [26]. Increasing Cu concentration generally results in a higher fraction of Al₂Cu. The solid solubility of Cu in α -Al increases as temperature increases from room temperature until 548 °C where the maximum solubility is reached, 5.65 mass% (maximum Cu that can be accommodated in α -Al in the form of solid solution in binary Al–Cu system) (Fig. 2a). Above 548 °C, however, the solubility of Cu decreases by increasing temperature [19]. Although increasing Cu up to 5.65 mass% provides formation of a higher fraction of Al₂Cu, at the same time, it

reduces the temperature gap between Al₂Cu formation and liquidus temperature (ΔT). Solution temperatures closer to liquidus temperature burden the complete dissolution of Al₂Cu with low risk of incipient melting. In fact, a certain gap between SHT temperature and liquidus line should be maintained. Therefore, a condition $\Delta T > 20$ °C was considered to choose optimal chemical composition. ΔT in property phase diagram is pointed out in Fig. 2c, and the values for each nominated chemical composition are collated in Table 1.

Introducing Mg to Al–Cu system enhances the response to ageing due to complex interactions between Mg atoms and vacancies [27]. Although high Mg level in the alloy is desired to intensify hardenability, it brings some difficulties for the SHT. Mg addition decreases the liquidus temperature as well as maximum solubility of Cu, and this subsequently reduces ΔT (Table 3). Moreover, generation of Mg-bearing intermetallic of S-Al₂CuMg which has a relatively lower melting temperature requires multi-step SHT to prevent overburning of such phase [28].

In previous studies on Al–Cu–Mg and Al–Cu–Mg–Ag alloys [16, 17, 20, 29], Mg level between 0.4 and 1.0 was typically used, while Cu/Mg was in the range 3–10. It was reported that increasing Mg content up to 1 mass% improves the hardenability in Al–Cu–Mg–Ag alloys [20]. It has been commonly agreed in the literature that the Cu/Mg ratio in the ternary Al–Cu–Mg system should exceed 5.6 in order to promote formation of thin-plate Al₂Cu, θ and Ω phases, which favours the mechanical properties [30].

Solidification simulation based on both equilibrium condition and Scheil equation showed that addition of only 0.2 mass% Mg to Al–Cu system induces the formation of

Table 2 Temperatures and time which were selected for SHT and artificial ageing for different alloys

Solidification rate/mm s ⁻¹	Alloys	Solution heat treatment				Artificial ageing	
		1st step		2nd step		T/°C	t/h
		T/°C	t/s	T/°C	t/h		
3	Al–Cu	–	–	520, 525	5, 10, 15, 20, 25	150, 180, 215	0.5, 1, 2, 4, 8, 16, 24, 64
	Al–Cu–Mg	–	–	510, 512, 515		175, 190, 215, 230	
	Al–Cu–Mg–Ag	–	–	510, 512, 515		150, 180, 215	
0.3	Al–Cu	–	–	520, 525, 530		150, 180, 215	
	Al–Cu–Mg	490, 495	1, 2, 5, 10, 20	510, 512, 515		175, 190, 215, 230	
	Al–Cu–Mg–Ag	485, 490	1, 2, 5, 10, 20	510, 512, 515		150, 180, 215	
0.03	Al–Cu	–	–	520, 525, 530		150, 180, 215	
	Al–Cu–Mg	490, 495	1, 2, 5, 10, 20	510, 512, 515		175, 190, 215, 230	
	Al–Cu–Mg–Ag	485, 490	1, 2, 5, 10, 20	510, 512, 515		150, 180, 215	

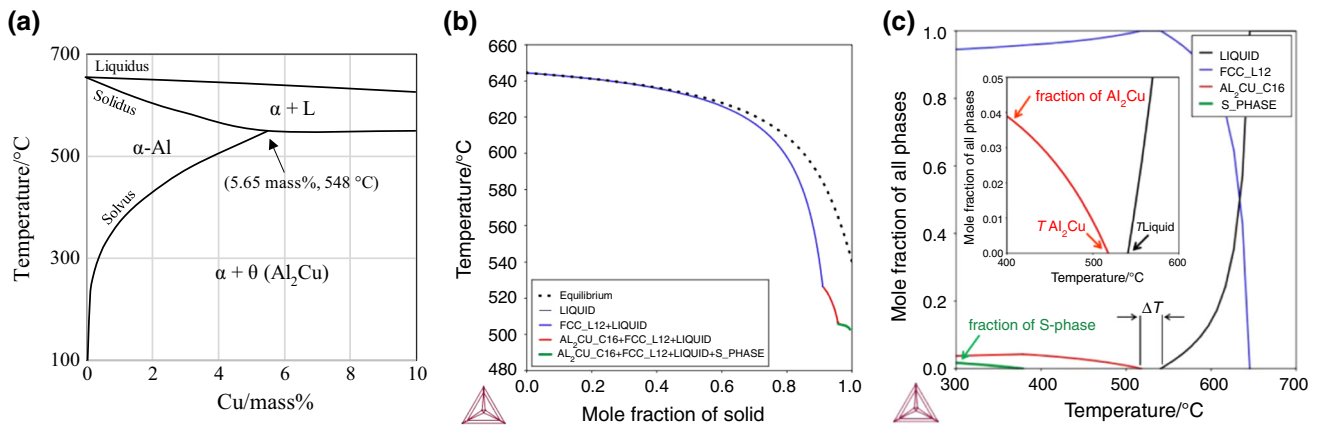


Fig. 2 **a** Reconstructed Al-rich end of the Al–Cu phase diagram according to [19]. **b** Equilibrium solidification (dashed line) vs. simulated solidification curve based on Scheil equation for Al–4.3Cu–0.7Mg–0.7Ag alloy. **c** Property phase diagram of Al–4.3Cu–0.7Mg alloy, corresponding fraction and temperature of phases based on equilibrium solidification

Table 3 Nominated chemical compositions, molar fraction of Al_2Cu and S- Al_2CuMg phases and corresponding temperature of phases calculated under equilibrium condition and based on Scheil equation

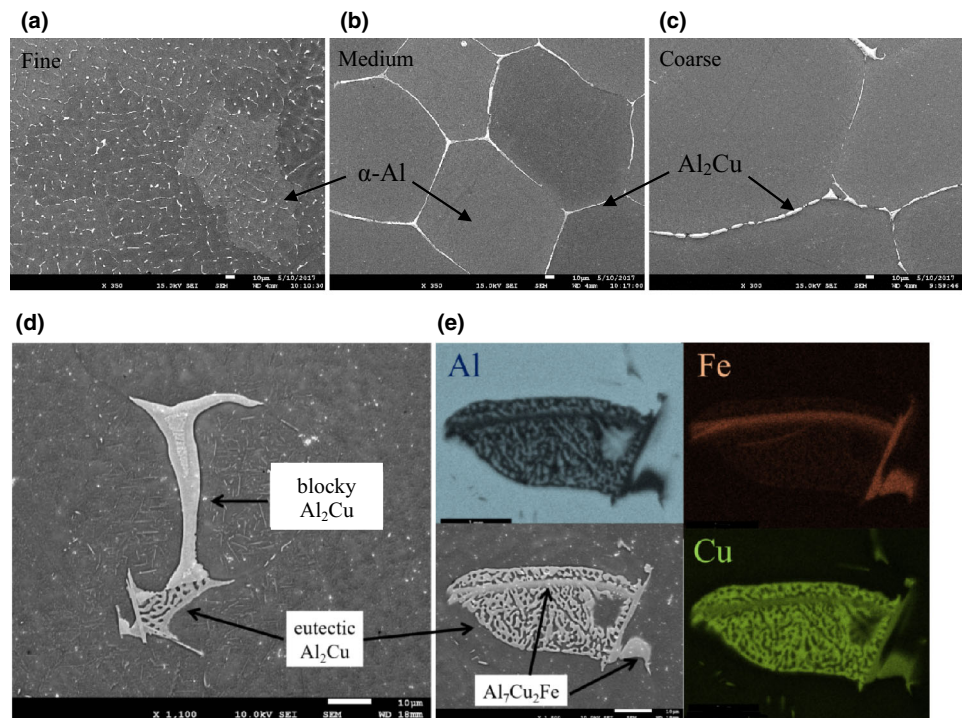
	Cu/Mg ratio	Solidification under equilibrium condition					Solidification based on Scheil equation				
		$\text{Al}_2\text{Cu}/\%$	$\Delta T/^\circ\text{C}$	$T_{\text{liquidus}}/^\circ\text{C}$	$T_{\text{Al}_2\text{Cu}}/^\circ\text{C}$	S phase/ $\%$	$\text{Al}_2\text{Cu}/\%$	$T_{\text{Al}_2\text{Cu}} \text{ start}/^\circ\text{C}$	$T_{\text{Al}_2\text{Cu}} \text{ end}/^\circ\text{C}$	S phase/ $\%$	$T_{\text{S-phase}}/^\circ\text{C}$
Al–5.7Cu	–	7.1	0	548	548	–	11.5	547	547	–	–
Al–4.7Cu	–	6.0	37	561	524	–	9.2	547	547	–	–
Al–4.3Cu	–	5.3	52	567	515	–	8.3	547	547	–	–
Al–4.0Cu	–	5.0	67	571	504	–	7.8	547	547	–	–
Al–4.3Cu–0.2Mg	21.5	5.5	36	556	519	< 0.1	3.7	542	508	1.0	509
Al–4.3Cu–0.3Mg	14.3	4.9	40	555	515	0.5	3.5	539	509	1.0	509
Al–4.3Cu–0.5Mg	8.6	4.2	30	547	517	1.5	3.0	533	508	1.8	508
Al–4.3Cu–0.7Mg	6.1	3.7	22	539	517	2.3	2.5	527	507	2.6	508
Al–4.3Cu–0.8Mg	5.4	3.2	16	536	520	2.8	2.1	525	508	3.1	508
Al–4.3Cu–1.0Mg	4.3	2.5	7	527	520	3.7	1.5	520	507	4.0	508
Al–4.5Cu–0.5Mg	9.0	4.5	22	542	520	1.5	3.1	534	508	1.9	509
Al–4.5Cu–0.7Mg	6.4	3.8	15	537	521	2.4	2.6	529	508	2.8	509
Al–4.5Cu–1.0Mg	4.5	2.8	0	525	525	3.8	1.7	521	508	3.6	508
Al–4.7Cu–0.5Mg	9.4	4.7	12	540	527	1.5	3.3	534	507	1.9	508
Al–4.7Cu–0.7Mg	6.7	4.1	6	533	526	2.4	2.8	529	508	2.8	508
Al–4.3Cu 0.7Mg–0.4Ag	6.1	4.1	24	540	516	2.3	2.4	527	506	1.2	506
Al–4.3Cu 0.7Mg–0.7Ag	6.1	4.1	25	540	515	2.3	2.4	526	506	1.2	506
Al–4.3Cu 0.7Mg–1.0Ag	6.1	4.1	25	540	515	2.3	2.4	526	506	1.2	505

S- Al_2CuMg phase in the as-cast microstructure. Equilibrium condition basically simulates solidification under very slow rate, while the Scheil equation is valid when the contribution from back diffusion is negligible [10] (Fig. 2). It was also understood that the fraction of S phase was

primarily a function of Mg content rather than Cu and Ag content (Table 3).

Two alloys of Al–4.3Cu–0.7Mg and Al–4.5Cu–0.5Mg have optimal composition with relatively high Cu content, sufficient ΔT and fairly low molar fraction of S- Al_2CuMg phase (1.5–2.6%). Al–4.3Cu–0.7Mg is preferred over the

Fig. 3 SEM micrographs of Al–Cu–Mg alloys with **a** 3, **b** 0.3 and **c** 0.03 mm s^{−1}. Solidification rates represent fine, medium and coarse microstructural scale, respectively. **d** Eutectic Al₂Cu, blocky Al₂Cu and **e** Al₇Cu₂Fe phase identified in the as-cast microstructure of the alloys



Al–4.5Cu–0.5Mg due to higher Mg content. In order to have a better comparison between Al–Cu–Mg and Al–Cu alloys, identical Cu content was chosen for Al–Cu system (e.g. Al–4.3Cu).

Evidence in the studies showed a range of 0.35–1.70 mass% Ag added to Al–Cu–Mg alloys to encourage Ω precipitation [20, 30–32]. Based on solidification simulation, Ag incorporation of 0.4–1.0 mass% into Al–4.3Cu–0.7Mg system changes neither any characteristic temperature of phases nor the fraction of phases (Table 3).

Bai et al. [32] reported a conclusive improvement in thermal stability of Ω which precipitates once Ag level increased from 0.4 to 0.8 mass%. In another study, where a varied set of compositions was studied to optimise precipitation hardening, the addition of 0.6 mass% Ag to Al–5Cu–1Mg alloy yielded the highest peak of hardness after ageing among the other Ag levels [20]. In the present study, according to the findings in other works, the addition of 0.7 mass% Ag was found a suitable amount to be added to Al–4.3Cu–0.7Mg in order to investigate the role of Ag addition on the heat treatment parameters.

Microstructure

SEM micrographs of Al–Cu, Al–Cu–Mg and Al–Cu–Mg–Ag alloys cast under different solidification rate are presented in Fig. 3. Principal microstructural constituents of alloys are α -Al and a continuous Cu-rich zone identified as

Al₂Cu phase (in the form eutectic phase and blocky phase (Fig. 3)). Limited traces of elongated Fe-rich intermetallics were also identified in the as-cast microstructures of all alloys, known as Al₇Cu₂Fe [33].

Solidification rate determines the microstructural scale (also known as the coarseness of microstructure). Increasing the solidification rate from 0.3 to 3 mms^{−1} resulted in a substantial reduction in the size of α -Al grain (Fig. 3). The average diameter of α -Al grains is reported in Table 4, where it can be understood that the size of grain increased by reducing the solidification rate irrespective of the alloy compositions. A continuous distribution of Al₂Cu particles was observed, from a few hundreds of microns to below fifty microns in length. Solute concentration of Cu, Mg and Ag in the centre of α -Al grains for the alloys under different as-cast conditions was measured using the WDS technique, and the average values are reported in Table 4. The average concentration of Cu in the matrix for Al–Cu alloy was lower for the case of high solidification rate (fine microstructural scale) compared to low ones (medium and coarse microstructural scales). A similar trend was found for Al–Cu–Mg and Al–Cu–Mg–Ag alloys (Table 4). Mg solute concentration, however, was found to be relatively higher in fine microstructure compared to coarser microstructure. Ag solute levels seem to be constant and equal to \sim 0.6 mass% in Al–Cu–Mg–Ag alloy irrespective of the microstructural scale.

Table 4 Average values of relevant microstructural features in the alloys with varied microstructural scale

Solidification rate/mm s ⁻¹	Microstructural scale	Alloys	Grain size/ μm	Solute concentration in the centre of α -Al grains/mass%		
				Cu	Mg	Ag
3	Fine	Al–Cu	15 \pm 1	1.4 \pm 0.2	–	–
		Al–Cu–Mg	11 \pm 1	1.5 \pm 0.2	0.6 \pm 0.1	–
		Al–Cu–Mg–Ag	17 \pm 4	1.5 \pm 0.2	0.60 \pm 0.1	0.60 \pm 0.1
0.3	Medium	Al–Cu	168 \pm 32	2.3 \pm 0.2	–	–
		Al–Cu–Mg	177 \pm 44	2.2 \pm 0.3	0.5 \pm 0.1	–
		Al–Cu–Mg–Ag	150 \pm 19	2.3 \pm 0.2	0.5 \pm 0.1	0.60 \pm 0.1
0.03	Coarse	Al–Cu	251 \pm 28	2.4 \pm 0.2	–	–
		Al–Cu–Mg	291 \pm 32	2.2 \pm 0.2	0.5 \pm 0.1	–
		Al–Cu–Mg–Ag	223 \pm 20	2.2 \pm 0.2	0.5 \pm 0.1	0.6 \pm 0.1

Solution heat treatment

Figure 4 shows typical DSC curves during heating for as-cast alloys with different microstructural scales. Al–Cu alloy showed a single endothermic peak, irrespective of microstructural scale, with an onset temperature of ~ 540 °C which corresponds to the melting of Al₂Cu phase [15]. Although Al₂Cu phase was identified in two different forms of eutectic and blocky phase (Fig. 3), both forms did not show separate peaks, which suggests the same melting temperature.

Unlike Al–Cu, both Al–Cu–Mg and Al–Cu–Mg–Ag with medium and coarse microstructural scale (solidification rate of 0.3 and 0.03 mm s⁻¹) showed multiple endothermic peaks; see peaks 2 and 3 pointed out in Fig. 4. Some specimens of both medium and coarse microstructure showed double peaks (peak 1 and 2), and others showed triple peaks (peaks 1, 2 and 3). Average onset temperature and area under peaks for each alloy are collated in Table 5. Peak 2 had an onset temperature between 489 and 501 °C, while peak 3 had an onset temperature of 494–508 °C. These peaks possibly correspond to the phases with lower melting temperatures compared to Al₂Cu, with onset temperatures between ~ 495 and ~ 513 °C relating to AlCuMg compounds (S-Al₂CuMg and Q-Al₇Cu₃Mg₆), reported in scholars [16, 17, 34]. Although these phases could not be identified using microscopic characterisation tools, DSC curve revealed their attendance. Solidification simulations based on thermodynamic calculations also revealed the presence of 1.2–2.6% S-Al₂CuMg phase in the as-cast microstructure. Under high solidification rate (3 mm s⁻¹), however, all alloys showed a single endothermic peak of melting Al₂Cu phase. In fact, it seems that high cooling rate arrested the formation of S-Al₂CuMg phase in cooling compositions of both Al–4.3Cu–0.7Mg and Al–4.3Cu–0.7Mg–0.7Ag. This consequently allows applying

one-step SHT even for Al–Cu–Mg and Al–Cu–Mg–Ag with fine microstructural scale.

Since the diffusion coefficient of Cu is much lower than Mg and Ag at the given temperatures, the homogenisation of solute within α -Al is controlled by the diffusion of Cu [35]. The Cu concentration in the centre of α -Al grains for Al–Cu alloy after various SHT times at 520 °C is presented in Fig. 5. The temperature of 520 °C was initially chosen for Al–Cu alloy due to having a reasonable gap of 20 °C with the onset temperature of melting Al₂Cu phase. For the case of fine microstructure (3 mm s⁻¹ solidification rate), a homogeneous Cu concentration of ~ 4.1 mass% in the α -Al matrix, close to the maximum Cu concentration of 4.33 mass% in Al–Cu alloy, was reached after only 10 h. According to equilibrium binary Al–Cu phase diagram (Fig. 2), the equilibrium Cu concentration in α -Al at 520 °C is equal to 4.55 mass%. After 10 h, Cu concentration was 3.2 and 3.0 mass% for medium and coarse microstructural scale with relatively large scatters. In fact, despite having quite similar onset temperature of melting Al₂Cu (~ 540 °C) in the different microstructural scales, the dissolution rate of Al₂Cu was significantly different. This is primarily attributed to different microstructural scales.

In medium and coarse microstructure, solute concentration did not reach 4.0 mass% even after 20-h exposure at 520 °C. Figure 6a, b shows the microstructure of solution-treated alloy after 10-h exposure at 520 °C with fine and medium microstructural scale. Considerable fraction of residual Al₂Cu was observed in medium microstructure, while negligible particles remained undissolved in the fine microstructure, which agrees with the higher solute concentration in the fine microstructure. The dissolution rate of Al₂Cu phases in α -Al is primarily a function of phase fraction, while homogenisation rate of Cu solute atoms is a function of diffusion distance, suggested by Sjölander et al.

Fig. 4 Typical DSC heating curves of as-cast alloys cast under different solidification rates (different microstructural scales). The curves have been offset for clarity

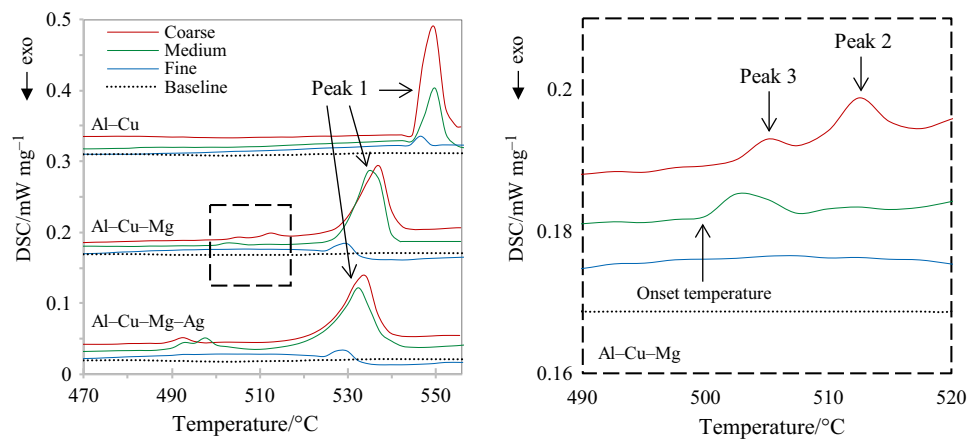


Table 5 Average onset temperature and area under endothermic peaks which are pointed out in Fig. 4

Solidification rate/mm s ⁻¹	Microstructural scale	Alloys	Onset temperature/°C			Area under peak/J g ⁻¹		
			Peak 1	Peak 2	Peak 3	Peak 1	Peak 2	Peak 3
3	Fine	Al-Cu	541	-	-	0.4	-	-
		Al-Cu-Mg	525	-	-	0.8	-	-
		Al-Cu-Mg-Ag	525	-	-	0.7	-	-
0.3	Medium	Al-Cu	540	-	-	5.1	-	-
		Al-Cu-Mg	526	508	501	8.4	0.2	0.1
		Al-Cu-Mg-Ag	526	495	490	9.3	0.3	0.2
0.03	Coarse	Al-Cu	541	-	-	8.3	-	-
		Al-Cu-Mg	528	508	500	8.3	0.2	0.1
		Al-Cu-Mg-Ag	528	494	489	9.4	0.3	0.2

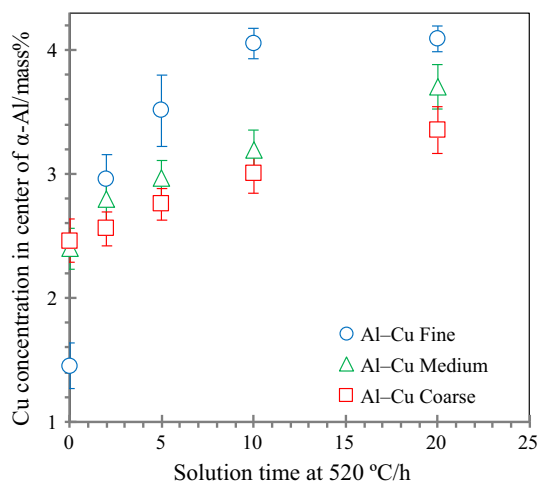
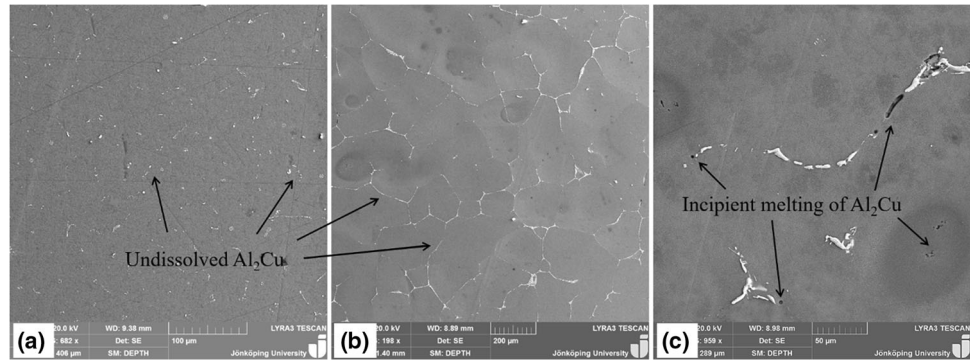


Fig. 5 Increment in Cu concentration in the centre of the α -Al grains for the Al-Cu alloy as a function of the solution treatment time

[10]. Han et al. [12] suggested different dissolution rates for eutectic Al_2Cu and block-like Al_2Cu phase where the former dissolves by fragmentation to smaller parts and

eventually dissolves by radial diffusion of Cu in the matrix, while the latter dissolves by spheroidisation and shrinkage. The author pointed out in another work that size and morphology of Al_2Cu phase influence dissolution rate where fine particles with lower aspect ratio dissolve faster than coarse elongated one [13]. In the present study, the comparison between the dissolution rates of Al_2Cu for different microstructural scales is not straightforward where the fast solidification rate resulted in dendritic growth of α -Al, while two slower solidification rates resulted in cellular growth (Fig. 3). Fine microstructure had relatively low Cu concentration profile (~ 1.5 mass%) in as-cast condition compared to two coarser microstructures (~ 2.3 mass%), which suggests a higher fraction of Al_2Cu phase is expected in the fine microstructure. Therefore, quite rapid dissolution rate of Al_2Cu in the fine microstructure despite considerably larger fraction compared with two other coarseness of microstructure is primarily due to exceptionally refined particles assisted by reduced diffusion distance (size of α -Al grains or interdendritic spacing).

Fig. 6 Microstructure of solution-treated Al–Cu alloy at 520 °C for 10 h with **a** fine and **b** medium microstructure. **c** Incipient melting pores formed in Al–Cu alloys with coarse microstructure during solution heat treatment at 530 °C after 10 h



Liu et al. [35] pointed out that homogenisation kinetic of Cu in α -Al has diverse relation with diffusion distance, which is in accordance with the experimental results of this study. Table 6 shows that applying identical SHT cycle to the Al–Cu alloy with medium and coarse microstructure resulted in rather similar Cu solute levels, while the Cu concentration was more scattered in the case of coarse microstructure compared with medium microstructure. This was similarly observed for Al–Cu–Mg and Al–Cu–Mg–Ag alloys, since the larger average diffusion distance in the coarse microstructure requires a reasonably long time for reaching a homogeneous distribution of Cu solutes.

Table 5 shows that despite the different microstructural scales in each alloy, the onset temperature of endothermic peaks is relatively similar. For instance, peak 1 in Al–Cu alloy has onset temperature of 540–541 °C for fine, medium and coarse microstructure. Albeit the magnitude of peaks significantly differed as a function of microstructural scale, the area under peaks of DSC curve with respect to a calorimetric constant is proportional to the enthalpy of the phase transformation. Figure 4 shows that the area under peak 1 is dramatically smaller in fine microstructure rather than medium and coarse ones irrespective of the alloy composition. Therefore, a fast dissolution rate of Al_2Cu in

fine microstructure is consistent with a lowered enthalpy of dissolution. In fact, refined continuous particles can be dissolved exchanging lower heat rather than coarser particles and elongated Al_2Cu networks. Therefore, proper dissolution temperature seems to be primarily influenced by the area under the peak rather than the onset temperature of the peaks.

The average Cu concentration in the centre of α -Al grains for Al–Cu alloy with coarse microstructural scale after SHT at 520 °C for 20 h was 3.0 mass%. Increasing SHT to 525 °C resulted in reasonably solutionised and homogenised microstructure after 20 h having Cu solute level of 4.05 ± 0.18 mass% in the matrix without noticeable numbers of overburnt phase. This is due to the immediate effect of SHT temperature on the diffusion rate which is magnified by raising the temperature [11]. Further increasing the SHT temperature to 530 °C resulted in frequent formation of incipient melting pores (Fig. 6c) without an indicative increase in the solute level (~ 4 mass%). A similar observation was found in fine microstructure once it was solution-treated at 525 °C compared to 520 °C. Therefore, a single-step SHT at 520 °C for 10 h is appropriate for fine microstructure, while medium and coarse microstructure needs a solution temperature of 525 °C for at least 20 h. Al_2Cu phase had somewhat lower melting

Table 6 Optimal solution heat treatment cycle and Cu solute level in Al matrix after solution heat treatment

Solidification rate/mm s ⁻¹	Microstructural scale	Alloys	Solution heat treatment	Cu in the α -Al after SHT/mass%
3	Fine	Al–Cu	520 °C for 10 h	4.08 ± 0.12
		Al–Cu–Mg	512 °C for 10 h	4.02 ± 0.12
		Al–Cu–Mg–Ag	512 °C for 10 h	4.05 ± 0.11
0.3	Medium	Al–Cu	525 °C for 20 h	4.04 ± 0.12
		Al–Cu–Mg	495 °C for 5 h + 512 °C for 20 h	4.10 ± 0.15
		Al–Cu–Mg–Ag	490 °C for 5 h + 512 °C for 20 h	3.99 ± 0.16
0.03	Coarse	Al–Cu	525 °C for 20 h	4.01 ± 0.21
		Al–Cu–Mg	495 °C for 5 h + 512 °C for 20 h	4.04 ± 0.25
		Al–Cu–Mg–Ag	490 °C for 5 h + 512 °C for 20 h	3.96 ± 0.22

temperature in Al–Cu–Mg and Al–Cu–Mg–Ag compared with Al–Cu alloy (Table 5). Therefore, lowered solution temperature of 510 °C applied for Al–Cu–Mg and Al–Cu–Mg–Ag alloys resulted in a small fraction of residual Al₂Cu. Heating at 515 °C on the other dissolved nearly all intermetallic Al₂Cu particles. Although a limited number of incipient melting pores were identified, a temperature in between 510 and 515 °C was chosen which resulted in a reasonable fraction (> 90%) of dissolved Al₂Cu without the occurrence of incipient melting. The optimised SHT for the alloys and final Cu solute level are summarised in Table 6. Applying single-step SHT on Al–Cu (fine, medium and coarse microstructure), Al–Cu–Mg (fine microstructure) and Al–Cu–Mg–Ag (fine microstructure) resulted in an average solute level of 4.0–4.1 mass%, while alloys possess ~ 4.3 mass% of Cu in their compositions (Table 1). The dissolution and homogenisation of Al₂Cu occurred rapidly in Al–Cu–Mg and Al–Cu–Mg–Ag with fine microstructure and were already seen for the Al–Cu alloy. Single-step SHT at 512 °C for 10 h for both Al–Cu–Mg and Al–Cu–Mg–Ag with fine microstructure is found to be suitable to dissolve Al₂Cu phase and homogenise Cu solute atoms over the matrix. The Cu solute levels in solution-treated condition reached 4.02 ± 0.12 and 4.05 ± 0.11 for Al–Cu–Mg and Al–Cu–Mg–Ag alloys, respectively. According to the equilibrium phase diagram, Cu has a maximum solubility of 4.70, 4.55 and 4.27 mass% in α -Al at 525, 520 and 512 °C, respectively. It means that Cu solute level in the alloy by applying single-step solution treatment might have not reached the maximum concentration value. Yet a reasonable fraction of 92–95% of the maximum solute level was obtained. However, complex solution treatments for similar alloys proposed in scholars, such as controlled heating [17] or multi-step solubilisation and homogenisation treatment [16], may assist in reaching solute levels closer to equilibrium values. DSC thermograms during heating for Al–Cu–Mg–Ag alloy with coarse microstructure in as-cast and solution-treated conditions (490 °C for 5 h + 512 °C for 20 h and quenched) are presented in Fig. 7b. Three distinct endothermic peaks, which represent the melting of Al₂Cu and AlCuMg phases, in the as-cast condition disappeared in the solution-treated condition. This is a further confirmation of fairly complete dissolution of such phases, which was also pointed out elsewhere [15].

The presence of phases with lower melting temperatures was identified in the DSC curves of Al–Cu–Mg and Al–Cu–Mg–Ag alloys having medium and coarse microstructures (Fig. 4). Al–Cu–Mg alloy with medium microstructural scale showed two peaks beside the peak related to Al₂Cu phase with an onset temperature of ~ 500 and ~ 508 °C. In order to dissolve phases corresponding to these peaks, the alloy was heated at 495 °C. This temperature has

sufficient temperature difference with an onset temperature of the peak 3 (~ 500 °C) and is commonly used during multi-step solution treatment similar to alloys in other studies [9, 17]. Cu concentration in different locals of α -Al grains as a function of distance to nearest Al₂Cu particles for different solution treatment times is presented in Fig. 7. Solid lines represent the linear trends of the concentration points. Severe Cu segregation exists across the α -Al in the as-cast condition. This was observed in medium and coarse microstructures of all alloys, which is due to the preferred distribution of the majority of θ -Al₂Cu in the grain boundary (Fig. 3). This finding was pointed out elsewhere [35].

An appreciable increase in Cu solute level was realised after 2-h SHT. It is presumed that this is due to the diffusion-controlled dissolution of Cu-containing phase with lower melting points (onset 500–508 °C) and migration of Cu solute into the matrix. SHT for longer time of 5 h and 20 h resulted in a marginal increase in solute level and still quite far from equilibrium Cu level at 495 °C. This suggests that diffusion rate at 495 °C is sluggish to dissolve Al₂Cu phase which has a higher melting point. Therefore, it is presumed that 2–5 h is the sufficient SHT time for the first step of SHT. In order to dissolve remained Al₂Cu phase, the first step of SHT (5 h at 495 °C) was followed by heating at 512 °C for 20 h which produced a quite homogenised matrix having an average solute level of 4.12 mass%. The similar treatment was carried out for Al–Cu–Mg–Ag alloy comprising medium and coarse microstructural scales giving similar results regarding Cu content in the matrix. The optimal SHT and Cu solute level in the Al matrix after SHT for each alloy are summarised in Table 6.

Artificial ageing

Hardness curves of solution-treated Al–Cu–Mg alloy with medium microstructural scale aged at different temperatures are illustrated in Fig. 8b. The peak hardness decreased as the ageing temperature was elevated from 190 to 215. Artificial ageing at 230 °C from 30 min to 64 h resulted in a monotonic decrease in the hardness without reaching any peak-age condition. Detecting no peak hardness at 230 °C is probably due to immediate coarsening of precipitates and over-ageing after 30-min exposure at relatively high temperature. The same finding for a similar alloy was reported during ageing at 220 °C in Ref. [20]. Figure 8a shows the DSC curves of the solution-treated alloys during heating. The exothermic peak of precipitation was identified, and onset temperature and peak temperature were marked for each curve. The onset temperature of the peak for Al–Cu–Mg alloy is 228 °C, meaning that

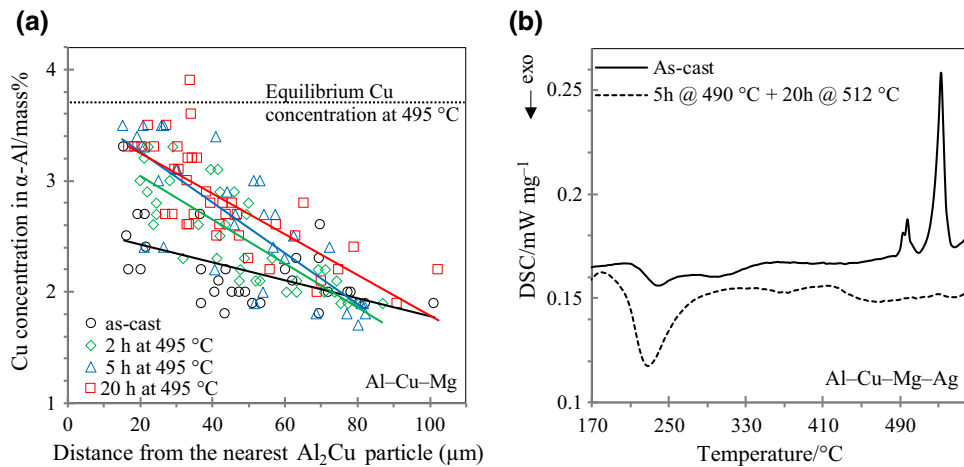
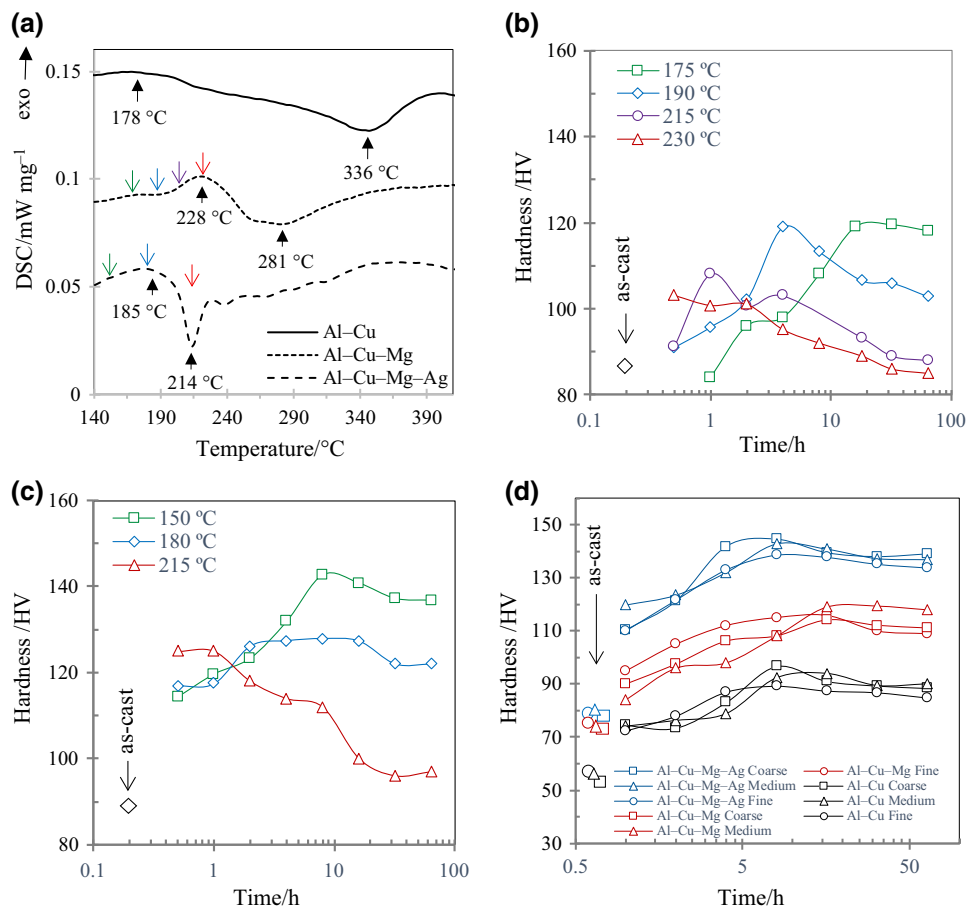


Fig. 7 **a** Cu concentrations measured within α -Al grains as a function of distance to the nearest Al_2Cu particle in the as-cast and solution-treated conditions. The alloy is Al-Cu-Mg with medium microstructural scale. The solid line represents the linear trends of the

concentration point, and the dash line shows the equilibrium Cu concentration at 495 °C for Al-4.3Cu-0.7Mg alloy. **b** DSC heating curves of as-cast and solution-treated Al-Cu-Mg-Ag alloy with coarse microstructure

Fig. 8 **a** DSC curves of solution-treated Al-Cu, Al-Cu-Mg and Al-Cu-Mg-Ag alloys with a medium microstructural scale during heating. Age-hardening curves of **b** Al-Cu-Mg and **c** Al-Cu-Mg-Ag alloys with medium microstructural scale. **d** Age-hardening curves of alloys with different microstructural scales for Al-Cu, Al-Cu-Mg and Al-Cu-Mg-Ag alloys aged at 150, 175 and 150 °C, respectively



precipitation already began once the temperature reached 230 °C. This supports rapid formation and coarsening of precipitates at 230 °C. The peak hardness of 119 Vickers was reached during ageing at 175 and 190 °C; meanwhile, the peak-aged time decreased from 16 h to 4 h. It seems

that a temperature range of 30–50 °C below the precipitation onset temperature is the sufficient temperature to reach peak-ageing in Al-Cu-Mg alloy. The shape of the thermograph peak of precipitation changes significantly by introducing Mg and Ag to the alloy. The precipitation

Table 7 Time to reach the hardness peak and average age-hardening response of the alloys with diversified microstructural scale

Alloy	Solidification rate/mm s^{-1}	Time to peak/h			Hardening response ^a (Vickers)		
		150 °C	180 °C	215 °C	150 °C	180 °C	215 °C
Al–Cu	3	4–8	2–4	< 0.5	37 ± 2	34 ± 4	20 ± 1
	0.3	8–16	2–4	< 0.5	37 ± 2	32 ± 2	23 ± 1
	0.03	8–16	1–4	< 0.5	41 ± 3	36 ± 3	23 ± 2
Al–Cu–Mg	175 °C	215 °C	230 °C	175 °C	215 °C	230 °C	
	3	4–16	< 1	< 0.5	44 ± 4	30 ± 4	25 ± 2
	0.3	8–16	< 1	< 0.5	42 ± 2	30 ± 2	22 ± 2
	0.03	8–16	1–2	< 0.5	42 ± 2	28 ± 2	26 ± 1
Al–Cu–Mg–Ag	150 °C	180 °C	215 °C	150 °C	180 °C	215 °C	
	3	8–16	2–4	< 0.5	63 ± 3	45 ± 4	36 ± 1
	0.3	8–16	2–4	< 0.5	62 ± 4	44 ± 2	39 ± 2
	0.03	4–8	2–4	< 0.5	60 ± 3	38 ± 3	32 ± 2

^aAge-hardening response is the difference in hardness between the peak-aged condition and as-cast condition

kinetic in Al–Cu alloy seems to be rather sluggish where there is a prolonged temperature difference of 158 °C between the onset temperature and peak temperature (178 and 336 °C) (Fig. 8a). At the same time, the temperature difference is 53 and 29 °C for Al–Cu–Mg and Al–Cu–Mg–Ag, respectively. Precipitation in Al–Cu–Mg alloy occurred at a lower temperature compared with Al–Cu–Mg–Ag alloy (Fig. 8a). Artificial ageing at 215 °C resulted in peak hardness after 1 h in Al–Cu–Mg alloy, while no peak was detected in Al–Cu–Mg–Ag. This suggests that 215 °C is a relatively high temperature for artificial ageing of Al–Cu–Mg–Ag alloy where the precipitation commenced at 185 °C; see precipitation onset temperature of Al–Cu–Mg–Ag alloy in Fig. 8a. At 150 °C, however, the alloys reached the peak-ageing condition (144 HV) in 8 h which is in the range of 130–170 Vickers reported in the studies for the similar alloy [20, 23, 36]. In another study [36], ageing of Al–4Cu–0.3Mg–0.4Ag alloy at 165 °C yielded 5% higher hardness peak than 200 °C. Another study documented that ageing at 160 °C always resulted in higher hardness peak compared to ageing at 190 and 220 °C for varied Al–Cu–Mg–Ag compositions [20]. This is in agreement with the finding that a proper ageing temperature to reach the peak-aged within the sufficient time needed to be at least 30 °C lower than onset temperature of precipitation. The similar range was also identified for Al–Cu alloy despite a relatively weak-hardening response (Fig. 8d).

Table 7 summarises the time to the peak-aged and average age-hardening response (the difference in hardness between the peak-aged condition and as-cast condition) at different temperatures for the alloys having varied microstructural scale. In Al–Cu–Mg alloy, elevating ageing

temperature constantly decreases both the time to the peak-aged and age-hardening response irrespective of microstructural scale. This similar behaviour is also pointed out for Al–Cu and Al–Cu–Mg–Ag alloy. Therefore, the highest hardness values are achieved at 150, 175 and 150 °C for Al–Cu, Al–Cu–Mg and Al–Cu–Mg–Ag alloys, respectively.

Figure 8d shows that as-cast Al–Cu–Mg has sustainably higher hardness compared to as-cast Al–Cu alloy. This is primarily due to further solid solution strengthening by 0.7 Mg addition where the average concentration of 0.5–0.6 mass% is found in α -Al matrix (Table 4). Addition of 0.7 Mg improved the age-hardening response without a significant change in the time required to reach the hardness peak. It is worthwhile to be noted that Al–Cu alloy reached the highest hardness peak at 150 °C, while Al–Cu–Mg alloy exhibited the highest hardness peak at 175 °C (Table 7).

Addition of 0.7 mass% Ag to Al–Cu–Mg alloy does not yield further hardness improvement in the as-cast condition. However, hardness significantly improved upon heat treatment in the presence of Ag. Ag addition meaningfully increased the age-hardening response from 46 to 66 Vickers. The Al–Cu–Mg–Ag exhibits quite rapid precipitation hardening, while hardening rate is relatively slower in Al–Cu and Al–Cu–Mg alloys. This was also reflected in sharper precipitation peak in the DSC curves of Al–Cu–Mg–Ag (Fig. 8a). The mild rise in the hardness in under-aged step for Al–Cu alloy is due to the precipitation of GP zones. By the addition of Ag, this stage disappears and the initial hardening rate increases. It has been reported that the addition of Ag promotes the precipitation of Ω phase,

thereby suppressing the precipitation of GP zones and θ' phase [23]. The increased hardening response might also be associated with Mg–Ag co-clusters [34]. Hono et al. [26] showed that co-clustering of Ag and Mg atoms during precipitation occurs after ageing for 15 s at 180 °C which explains the immediate hardening response due to the presence of Ag.

Figure 8d presents the variation of hardness versus ageing time for alloys with different microstructural scales. The artificial ageing temperature is 150, 175 and 150 °C for Al–Cu, Al–Cu–Mg and Al–Cu–Mg–Ag, respectively, which resulted in the highest hardness peak. It seems that the microstructural scale does not have pronounced effect either on time to peak-aged or on peak hardness values irrespective of the alloy composition. The artificial ageing responses are rather similar for the different microstructural scales of each alloy (Table 7). In a study, where artificial ageing of Al–Si–Cu–Mg cast alloy was investigated [25], the ageing response was weakly dependent on the coarseness of the microstructure which is consistent with ageing behaviour of Al–Cu–(Mg–Ag) alloys studied in this work.

Conclusions

1. Solidification simulations under equilibrium condition and Scheil equation show that Cu/Mg ratio in Al–Cu–(Mg–Ag) controls melting temperature of Al_2Cu phase, the liquidus temperature and the fraction of Al_2Cu and S- Al_2CuMg phases. Cu/Mg equal to ~ 6.1 with Cu content of 4.3 mass% is one of the optimal combinations suitable for solution heat treatment process where overburning temperature of phases is a critical parameter.
2. The as-cast microstructural scale of Al–Cu–(Mg–Ag) alloys has a remarkable influence on the dissolution rate of Al_2Cu and homogenisation kinetic of Cu in α -Al. Refined microstructure (α -Al grain $< 20 \mu\text{m}$) requires 10 h to dissolve Al_2Cu into the α -Al and to reach a homogenised Cu solute concentration over the α -Al matrix through a single-step solution treatment. Coarse microstructures (grain size ~ 150 – $300 \mu\text{m}$), however, need at least 25 h through a double-step solution treatment to reach reasonably homogenised structure without the formation of noticeable incipient melting pores. The homogenisation time is solely influenced by the microstructural scale irrespective of chemical composition. However, optimal solution temperature is a function of chemical compositions where the addition of Mg to Al–Cu decreased the solutionising temperature.
3. The artificial ageing response is independent of the microstructural scale as long as the microstructure is homogenised and solutionised before ageing. Elevating the artificial ageing temperature reduces the peak-aged time and degrades the peak hardness. Suitable temperature to reach the peak-ageing condition within a reasonable time (< 20 h) needed to be sufficiently lower than the onset temperature of precipitation. The elevated temperature of artificial ageing drastically degrades the peak of hardness. Addition of Ag to Al–Cu–Mg yields a noticeable improvement in the hardness values.

Acknowledgements Open access funding provided by Jönköping University. The work is funded by SIP Lättvikt, a collaboration between Vinnova, Formas and the Swedish Energy Agency, Grant No. 2016-04330. GKN Aerospace and RISE SWECAST are acknowledged for advisory support. Mr. Andrea Montesi is acknowledged for technical assistance.

Open Access This article is distributed under the terms of the Creative Commons Attribution 4.0 International License (<http://creativecommons.org/licenses/by/4.0/>), which permits unrestricted use, distribution, and reproduction in any medium, provided you give appropriate credit to the original author(s) and the source, provide a link to the Creative Commons license, and indicate if changes were made.

References

1. Polmear I. Aluminium alloys—a century of age hardening. In: Nie JF, Morton AJ, Muddle BC, editors. *Materials forum*, vol 28. 2004.
2. Kaufman JG, Rooy EL. *Aluminum alloy castings: properties, processes, and applications*. Materials Park: Asm International; 2004.
3. Kobayashi T. *Strength and toughness of materials*. Berlin: Springer; 2012.
4. Zolotarevsky VS, Belov NA, Glazoff MV. *Casting aluminum alloys*, vol. 12. Oxford: Elsevier; 2007.
5. Vietz J, Polmear I. The influence of small additions of silver on the ageing of aluminium alloys. *Observations on Al–Cu–Mg alloys*. *Inst Met J*. 1966;94(12):410–9.
6. Callister WD, Rethwisch DG. *Fundamentals of materials science and engineering: an integrated approach*. Hoboken: Wiley; 2012.
7. Ringer S, Sakurai T, Polmear I. Origins of hardening in aged Al–Cu–Mg–(Ag) alloys. *Acta Mater*. 1997;45(9):3731–44.
8. Muddle BC, Polmear I. The precipitate Ω phase in Al–Cu–Mg–Ag alloys. *Acta Metall*. 1989;37(3):777–89.
9. Liu D, et al. Microstructural evolution and tensile mechanical properties of thixoformed high performance aluminium alloys. *Mater Sci Eng, A*. 2003;361(1):213–24.
10. Sjölander E, Seifeddine S. Optimisation of solution treatment of cast Al–Si–Cu alloys. *Mater Des*. 2010;31:S44–9.
11. Sjölander E, Seifeddine S. Optimization of solution treatment of cast Al–7Si–0.3Mg and Al–8Si–3Cu–0.5Mg alloys. *Metall Mater Trans A*. 2014;45(4):1916–27.
12. Han Y, et al. 08-014 effect of solution heat treatment type on the dissolution of copper phases in Al–Si–Cu–Mg type alloys. *Trans Am Foundrymen's Soc*. 2008;116:79.

13. Zamani M, Seifeddine S, Jarfors AE. High temperature tensile deformation behavior and failure mechanisms of an Al–Si–Cu–Mg cast alloy—the microstructural scale effect. *Mater Des.* 2015;86:361–70.
14. Liu D, et al. Microstructural evolution and tensile mechanical properties of thixoformed high performance aluminium alloys. *Mater Sci Eng, A.* 2003;361(1–2):213–24.
15. Masuku E et al. Optimisation of the solution heat treatment of rheo-processed Al–Cu–Mg–(Ag) alloys A206 and A201. In: Dargusch MS, Keay SM, editors. *Materials science forum*, vol 618–9. Zurich: Trans Tech Publications Ltd; 2009.
16. Möller H, Govender G. editors. The heat treatment of rheo-high pressure die cast Al–Cu–Mg–Ag alloy 2139. In: *Solid state phenomena*, vol 192–3. Zurich: Trans Tech Publications Ltd; 2013.
17. Daswa P, Möller H, Govender G. Optimization of the solution heat treatment of rheo-high pressure die cast Al–Cu–Mg–Ag 2139 alloy. In: Chikwanda HK, Chikosha S, editors. *Materials science forum*, vol 828–9. Zurich: Trans Tech Publications Ltd; 2015.
18. Sjölander E, Seifeddine S. The heat treatment of Al–Si–Cu–Mg casting alloys. *J Mater Process Technol.* 2010;210(10):1249–59.
19. Sun D, et al. Thermoelectric power characterization of a 2024 aluminum alloy during solution treatment and aging. *Mater Charact.* 1996;36(2):83–92.
20. Al-Obaisi A, et al. Precipitation hardening and statistical modeling of the aging parameters and alloy compositions in Al–Cu–Mg–Ag alloys. *J Mater Eng Perform.* 2016;25(6):2432–44.
21. Reich L, Murayama M, Hono K. Evolution of Ω phase in an Al–Cu–Mg–Ag alloy—a three-dimensional atom probe study. *Acta Mater.* 1998;46(17):6053–62.
22. Masuku E et al. Rheocasting of Al–Cu alloy A201 with different silver contents. In: Hirt G, Rassili A, Bührig-Polaczek A, editors. *Solid state phenomena*, vol 141–3. Zurich: Trans Tech Publications Ltd; 2008.
23. Li Y, et al. Enhanced mechanical properties in an Al–Cu–Mg–Ag alloy by duplex aging. *Mater Sci Eng, A.* 2011;528(28):8060–4.
24. Olofsson J, et al. Characterisation and investigation of local variations in mechanical behaviour in cast aluminium using gradient solidification, Digital Image Correlation and finite element simulation. *Mater Des.* 2014;56:755–62.
25. Sjölander E, Seifeddine S. Artificial ageing of Al–Si–Cu–Mg casting alloys. *Mater Sci Eng, A.* 2011;528(24):7402–9.
26. Hono K, Sakurai T, Polmear I. Pre-precipitate clustering in an Al–Cu–Mg–Ag alloy. *Scr Metall Mater.* 1994;30(6):695–700.
27. Katgerman L, Eskin D. Hardening, annealing, and aging. In: Totten GE, MacKenzie DS, editors. *Handbook of aluminum, physical metallurgy and processes.* London: CRC; 2003. p. 259–303.
28. Birbilis N, et al. Nano-scale dissolution phenomena in Al–Cu–Mg alloys. *Electrochem Commun.* 2008;10(1):32–7.
29. Liu XY, et al. Effects of solution treatment on the microstructure and mechanical properties of Al–Cu–Mg–Ag alloy. *Mater Des.* 2010;31(9):4392–7.
30. Bakavos D, et al. The effect of silver on microstructural evolution in two 2xxx series Al-alloys with a high Cu: Mg ratio during ageing to a T8 temper. *Mater Sci Eng, A.* 2008;491(1–2):214–23.
31. Bai S, et al. Atom probe tomography study of Mg-dependent precipitation of Ω phase in initial aged Al–Cu–Mg–Ag alloys. *Mater Sci Eng, A.* 2015;637:183–8.
32. Bai S, et al. Effects of Ag variations on the microstructures and mechanical properties of Al–Cu–Mg alloys at elevated temperatures. *Mater Sci Eng, A.* 2014;611:69–76.
33. Roy S, et al. Comparative evaluation of cast aluminum alloys for automotive cylinder heads: part I—microstructure evolution. *Metall Mater Trans A.* 2017;48(5):2529–42.
34. Liu XY, et al. Microstructure and mechanical properties of Al–Cu–Mg–Mn–Zr alloy with trace amounts of Ag. *Mater Sci Eng, A.* 2009;525(1–2):128–32.
35. Liu XY, et al. Microstructural evolution of Al–Cu–Mg–Ag alloy during homogenization. *J Alloy Compd.* 2009;484(1–2):790–4.
36. Liu XY, et al. Effect of aging temper on the thermal stability of Al–Cu–Mg–Ag heat-resistant alloy. *Mater Des.* 2013;46:360–5.

Publisher's Note Springer Nature remains neutral with regard to jurisdictional claims in published maps and institutional affiliations.